

Serveur Académique Lausannois SERVAL serval.unil.ch

Author Manuscript

Faculty of Biology and Medicine Publication

This paper has been peer-reviewed but does not include the final publisher proof-corrections or journal pagination.

Published in final edited form as:

Title: Inadequate T follicular cell help impairs B cell immunity during HIV infection.

Authors: Cubas RA, Mudd JC, Savoye AL, Perreau M, van Grevenynghe J, Metcalf T, Connick E, Meditz A, Freeman GJ, Abesada-Terk G Jr, Jacobson JM, Brooks AD, Crotty S, Estes JD, Pantaleo G, Lederman MM, Haddad EK

Journal: Nature medicine

Year: 2013 Apr

Volume: 19

Issue: 4

Pages: 494-9

DOI: 10.1038/nm.3109

In the absence of a copyright statement, users should assume that standard copyright protection applies, unless the article contains an explicit statement to the contrary. In case of doubt, contact the journal publisher to verify the copyright status of an article.



Published in final edited form as:

Nat Med. 2013 April ; 19(4): . doi:10.1038/nm.3109.

Inadequate T follicular cell help impairs B cell immunity during HIV infection

Rafael A. Cubas¹, Joseph C. Mudd², Anne-Laure Savoye³, Matthieu Perreau³, Julien van Grevenynghe¹, Talibah Metcalf¹, Elizabeth Connick⁴, Amie Meditz⁴, Gordon J. Freeman⁵, Guillermo Abesada-Terk Jr.⁶, Jeffrey M. Jacobson⁷, Ari D. Brooks⁸, Shane Crotty^{9,10}, Jacob D. Estes¹¹, Giuseppe Pantaleo³, Michael M. Lederman², and Elias K. Haddad¹

¹Vaccine and Gene Therapy Institute of Florida, Port St. Lucie, Florida, USA ²Division of Infectious Diseases, Center for AIDS Research, Case Western Reserve University/University Hospitals, Case Medical Center, Cleveland, Ohio, USA ³Divisions of Immunology and Allergy, Swiss Vaccine Research Institute, Lausanne University Hospital, University of Lausanne, Lausanne, Switzerland ⁴Division of Infectious Diseases, University of Colorado Denver, Colorado, USA ⁵Department of Medical Oncology, Dana-Faber Cancer Institute, Harvard Medical School, Boston, Massachusetts, USA ⁶Robert and Carol Weissman Cancer Center, Martin Memorial Health Systems, Stuart, Florida, USA ⁷Division of Infectious Diseases and HIV Medicine, Drexel University College of Medicine, Philadelphia, Pennsylvania, USA ⁸Department of Surgery, Drexel University College of Medicine, Philadelphia, Pennsylvania, USA ⁹Division of Vaccine Discovery, La Jolla Institute for Allergy and Immunology (LIAI), La Jolla, California, USA ¹⁰Center for HIV/AIDS Vaccine Immunology and Immunogen Discovery (CHAVI-ID) ¹¹The AIDS and Cancer Virus Program, SAIC-Frederick, National Cancer Institute, NIH, Frederick, Maryland, USA

Abstract

The majority of HIV infected individuals fail to produce protective antibodies and have diminished responses to immunization¹⁻³. We report that even though there is an expansion of T follicular helper (Tfh) cells in HIV infected individuals, these are unable to provide adequate B cell help. A higher frequency of PD-L1⁺ germinal center (GC) B cells from lymph nodes of HIV infected individuals suggested a potential role for PD-1/PD-L1 interaction in regulating Tfh cell function. In fact, engagement of PD-1 on Tfh cells led to a reduction in cell proliferation, activation, ICOS expression and IL-21 cytokine secretion. Importantly, blocking PD-1 signaling enhanced HIV-specific immunoglobulin production *in vitro*. We further show that at least part of this defect involves IL-21 as addition of this cytokine rescued antibody responses and plasma cell generation. Our results suggest that deregulation of Tfh-mediated B cell help diminishes B cell responses during HIV infection and may be related to PD-1 triggering on Tfh cells. These results show, for the first time, a role for Tfh cell function in HIV pathogenesis and suggest that an alteration in their function could have a significant impact on the outcome and control of HIV infection, future infections and vaccinations.

Author Contributions

R.A.C. designed and performed experiments, analyzed data and wrote the manuscript; J.M., helped perform the phenotyping of Tfh and LN cell populations. A.L.S and M.P. helped provide preliminary data and performed the Luminex assays. J.vG. helped in the coculture assays and ELISAs. T.M assisted in the tonsil processing. L.Z provided tissue sections for IHC; G.F provided valuable reagents and intellectual input. J.J., provided LN samples and discussion. GA provided intellectual input and valuable tonsil samples. S.C., assisted in experimental design, discussion and analysis of data. J.E. performed IHC, G.P. and M.L., provided valuable discussion, designed experiments, provided conceptual advice and edited the manuscript. E.K.H., conceived and directed the research, analyzed data and helped write the manuscript.

Competing Financial Interests

The authors declare no competing financial interests.

During HIV infection there is a profound deregulation in B-cell function^{4–6}. However, little is known about the underlying mechanisms that alter B cell responses and antibody production at the site of their origin, the lymphoid tissues. The dynamic interplay between Tfh cells and GC B cells is essential in establishing protective humoral immune responses. Furthermore, the rare and broad neutralizing anti-HIV antibodies against different strains of HIV are enriched with somatic hypermutations^{7–9}, a property that is largely the result of Tfh interaction with GC B cells. It has further been shown, in the LCMV mouse model, that sustained Tfh function is required to control persistent viral infection^{10,11}. Preserving and enhancing Tfh function could therefore prove imperative in promoting efficient humoral defenses against HIV and improving the outcome of vaccination in infected patients.

We studied lymph node mononuclear cells (LNMCs) from healthy controls and ART-naïve, HIV-1-infected subjects (CD4 T-cell count > 350 per mm³ and plasma HIV RNA levels > 2000 copies ml⁻¹) (Supplementary Table. 1). Initial characterization demonstrated a significant increase ($P=0.0012$) in the frequency of Tfh cells in HIV-infected LNs (Fig. 1a) and more than 90% of these cells expressed Bcl-6, the master regulator for Tfh cells, and PD-1, confirming their Tfh identity (Supplementary Fig. 1a–c)¹². No significant differences were observed in the naïve, central memory or effector memory CD4⁺ T cell compartments (Fig. 1a) (Supplementary Fig. 2 for gating strategies). We also observed a significant increase ($P<0.0003$) in the frequency of GC B cells and a significant reduction ($P<0.02$) in the frequency of memory B cells in HIV-infected LNs (Fig. 1b). These results indicate that in HIV-infected LNs there is an expansion of Tfh cells and GC B cells likely driven by chronic infection and antigen accumulation within the follicular microenvironment^{13,14}. These results are in accordance with recently published reports in humans¹⁵ and macaques^{16,17}.

To investigate whether the function of Tfh cells is affected during HIV infection, we generated an *in vitro* coculture system in which sorted Tfh and non-Tfh cells are placed in coculture with sorted autologous GC-enriched B cells in the presence of staphylococcal enterotoxin B (SEB). This coculture system allows for the quantification of Tfh-mediated B cell help by measuring the accumulation of immunoglobulin in the culture supernatant and the absolute numbers of live cells at different time points (Supplementary Fig. 3a, b). Using this assay we found that cocultures from HIV⁺ LNs had a 92% reduction in the levels of IgG when compared to cocultures from control LNs (Fig. 1c, d). This reduction was also observed in cocultures from SIV⁺ macaques (Supplementary Fig. 4a). The absolute number of live B cells and Tfh cells was also significantly ($P<0.01$ and $P<0.02$) reduced after 7 d in coculture (Fig. 1e, f). A decrease in the levels of IL-10 was also observed in cocultures from HIV⁺ subjects (Supplementary Fig. 5). We were unable, however, to quantify the levels of IL-21 in the supernatants likely due to its rapid consumption. These results suggest that in LNs from HIV⁺ individuals, Tfh cell function is altered and this affects B cell survival and antibody production.

We next explored the phenotype of Tfh cells in HIV-infected and uninfected LNs. Tfh cells from HIV⁺ and control LNs expressed similar levels of Bcl-6, ICOS, CD40L and PD-1 (Fig. 2a, b and Supplementary Fig. 6). Tfh cells sorted from infected and uninfected LNs secreted similar levels of cytokines including IL-4, IL-10 and IL-21. In fact, we observed a tendency towards higher IL-21 production in Tfh cells from HIV-infected individuals (Supplementary Fig. 7). Thus, Tfh cells from both infected and uninfected LNs appear to be phenotypically similar suggesting that the alteration in Tfh cell function observed in the cocultures could arise from their interaction with B cells.

Since HIV infection is known to affect intrinsic B cell function^{4,18,19}, we investigated the status of LN resident B cells. Naïve, GC and memory B cells from LNs of HIV⁺ subjects expressed higher levels of CD95 than their counterparts from control LNs suggesting an increased propensity to apoptosis (Supplementary Fig. 8a, b). We next examined the capacity of B cells to survive without any T cell help and to produce immunoglobulin following polyclonal stimulation with CpG-B²⁰. We showed that GC-enriched B cells from HIV⁺ LNs produced similar levels of IgG to those from control LNs (Supplementary Fig. 9a). The viability of these cells was reduced, but not significantly, in HIV infected LN (Supplementary Fig. 9b). We also observed a tendency towards reduced levels of IL-6 from GC-enriched B cells from HIV⁺ LNs (Supplementary Fig. 9c) which could impact IL-21 secretion from Tfh cells²¹.

Since Tfh cells express high levels of the negative regulator PD-1 we next investigated whether expression of its ligands was increased in B cell subsets from HIV⁺ LNs. A significantly ($P = 0.015$) higher frequency of GC B cells from HIV⁺ LNs expressed PD-L1 (Fig. 2c). This was specific for GC B cells as naïve, early memory and late memory B cells showed a similar frequency of PD-L1 expression. We did not observe any differences in PD-L2 expression (Fig. 2d). Importantly, staining of LN tissue sections from HIV⁺ subjects showed an abundant expression of PD-L1 within the follicles (Fig. 2e). The levels of PD-L1 expression within the GC area were noticeably higher in LNs from HIV⁺ individuals and this was also the case for LN samples from SIV-infected macaques. These results suggest that the increased frequency of PD-L1⁺ GC B cells could be affecting Tfh cell function.

We next examined whether PD-1 triggering on Tfh cells could result in functional alterations that could affect B cell help. Tfh cells from uninfected tonsils were sorted and cultured in the presence of anti-CD3, anti-CD28 and PD-L1 coated beads (PD-L1 beads) to trigger PD-1 in the context of T-cell receptor activation, or anti-CD3, anti-CD28 and isotype control coated beads (control beads) or left unstimulated. When Tfh cells were cultured in the presence of control beads there was a significant ($P < 0.001$) induction in Ki-67 and CD38 expression suggesting an increased proliferative capacity. However, stimulation with PD-L1 beads reduced the frequency of Ki-67⁺ and CD38⁺ Tfh cells (Fig. 3a). This was translated into a decrease in the frequency and absolute number of live Tfh cells (Fig. 3b). This reduction in Ki-67 expression was maintained after five days (Fig. 3c). Unexpectedly, triggering PD-1 also inhibited ICOS expression (Fig. 3d) which could affect IL-4 and IL-21 cytokine secretion²². In fact, PD-1 triggering led to a 60% decrease in the levels of IL-21 (Fig. 3e) and a 78% and 95% decrease in the levels of IL-4 and IL-10 respectively (Supplementary Fig. 10). These results suggest that PD-1 triggering on Tfh cells affects multiple central aspects of Tfh cell biology including cytokine secretion.

If PD-1 triggering on Tfh cells from HIV⁺ LNs could affect IL-21 secretion, that is critical for B cell survival and differentiation into plasma cells, then supplementation with IL-21 should restore and enhance antibody production. In fact, cocultures of Tfh cells from infected LNs showed a significant restoration in IgG production when supplemented with IL-21 to the levels observed in cocultures from control LNs (Fig. 4a, b). Addition of IL-21 increased the amount of IgG produced by B cells in the coculture and led to a dose-dependent increase in CD27 MFI on B cells suggesting the accumulation of plasma cells (Fig. 4c). IL-21 supplementation also led to an apparent increase in the absolute number of live B cells (Fig. 4d) in accordance with the ability of IL-21 to promote B cell differentiation, survival and proliferation in the context of B cell help²³.

We next determined whether exogenous IL-21 could enhance HIV-specific Tfh responses. Tfh cells and GC-enriched B cells were sorted and cultured with primed monocytes for seven days in the presence or absence of IL-21. Addition of IL-21 enhanced antigen specific

Tfh-mediated B cell responses (Fig. 4e). We also tested whether blocking PD-1 engagement with its ligands could restore antibody production. For this, Tfh cells, B cells and primed monocytes were cultured in the presence or absence of anti-PD-L1 and PD-L2 blocking antibodies or isotype control. Blocking PD-L1 and PD-L2 increased IgG production by 78% when compared to the isotype control group (Fig. 4f). As expected there was no increase in the levels of IgG when the PD-1 pathway was blocked in cocultures from uninfected subjects (Supplementary Fig. 11). Overall, these results highlight a potential role for PD-1 engagement and IL-21 in altering Tfh-mediated B cell help during HIV infection. They further indicate that interfering with PD-1 triggering could enhance HIV-specific humoral defenses that are compromised during HIV infection.

Even though Tfh cells from control and HIV⁺ LNs were phenotypically similar, the function of these cells is altered in the presence of B cells. Interestingly, in a mismatch coculture assay using Tfh and GC-enriched B cells before and after SIV infection (Supplementary Fig. 4b) we observed that only GC-enriched B cells from SIV⁺ macaques, which also express a higher frequency of PD-L1 (Fig. 2e), affected Tfh-mediated B cell responses and immunoglobulin production. These results reinforce the idea that the Tfh cells themselves are not dysfunctional, but rather, their function is affected once they come into contact with PD-L1 expressing B cells.

Here we propose a model in which HIV infection drives the expansion of both Tfh and GC B cells, but the heightened levels of activation and antigen overload likely increases the frequency of PD-L1⁺ GC B cells leading to excessive and persistent triggering of PD-1 on Tfh cells affecting their capacity to provide B cell help. This effect combined with B cell intrinsic defects, results in the inability to mount appropriate Tfh-mediated B cell responses. Even though HIV infected subjects show hypergammaglobulinemia, this likely arises from hyperactivated naïve B cells¹. Similarly, an increase in SIV-specific antibodies has been associated with the accumulation of Tfh cells¹⁷, but their level and function could be suboptimal preventing the generation of efficient antibody responses (magnitude and breadth). Alternatively, these SIV-specific antibodies could have been generated independently of Tfh cells. It is important to note that in this study we were unable to distinguish Tfh cells from T follicular regulatory (Tfr) cells which also express CXCR5 and which could affect Tfh-mediated B cell responses²⁴⁻²⁷. It will be important to determine their presence and function during HIV infection.

PD-L1 expression on B cells has been shown to negatively regulate Tfh cell expansion in mice²⁸. Here we show that PD-1 triggering affects Tfh cell function leading to reduced ICOS expression which could affect downstream transcription factors like c-Maf²⁹⁻³¹ and subsequently IL-4 and IL-21 cytokine secretion thereby affecting B cell help (Supplementary Fig. 12). It is known that the majority of HIV infected individuals have a delay in the generation and an absence of broadly neutralizing HIV-specific antibodies^{4,32,33}. To what extent the alteration in Tfh cell function has an impact on the timing of production and on the quality of neutralizing antibodies remains to be determined.

The signals leading to increased PD-L1 expression on GC B cells are unclear, but are likely the result of increased levels of interferons that can upregulate PD-L1 expression³⁴. Treatment of mice with blocking anti-PD-L1 or PD-1 antibodies has been shown to enhance Tfh cell expansion and function and increase the number of GC B cells, plasmablasts and antigen specific antibody responses^{28,35}. Similarly, PD-1 blockade in macaques improved humoral responses and increased SIV specific antibody responses³⁶. Our work, together with these studies, suggests a critical role for the PD-1 pathway in regulating Tfh cell function. Because of persistent PD-L1 expression on GC B cells, Tfh cells in HIV infected subjects may lose their ability to properly generate *de novo* humoral responses to new

infections and their ability to respond to vaccinations. Consistent with this are the reduced levels in antibody responses to Hepatitis B, measles, mumps and rubella vaccines in HIV⁺ subjects^{2,37,38}. Overall, our results suggest that for effective vaccination of HIV-infected individuals, the proper function of Tfh cells needs to be considered.

Online Methods

Study subjects

All procedures were approved by the Institutional Review Boards at the relevant institutions, and all participants gave written informed consent before all procedures. Whole pelvic lymph nodes were obtained from adult women not known to be HIV-1 infected who were undergoing medically indicated surgery at University Hospitals of Cleveland. Their average age was 53 ± 14 years. ART-naïve HIV-1-infected individuals were recruited at the Drexel University College of Medicine (Philadelphia, PA). Average age of these subjects was 43 ± 13 years. All were naïve to ARV therapy and had HIV-1 RNA levels in their plasma 2000 copies ml^{-1} . The CD4⁺ T cell count in these subjects was 514 ± 120 cells ml^{-1} . Lymph nodes were excised from the inguinal region under local anesthesia as described previously³⁹. Surgeries were performed in the morning and the excised nodes were then placed in RPMI medium and shipped to Case Western Reserve University at 4 °C via same day air along with matching peripheral blood. The time between biopsy and subsequent specimen processing was no more than 7 hours.

We analyzed 2 Rhesus macaques longitudinally pre-infection and during chronic infection. Rhesus macaques (Indian origin *Macaca mulatta*; RMs) were seronegative for simian retrovirus type D, simian T-cell lymphotropic virus, and SIV at study initiation and did not express protective MHC-I alleles (MamuB*08, MamuB*17). RMs were infected with either SIVmac239 or SIVsmE660. Peripheral lymph node biopsies were obtained before infection and during chronic infection. Animals were housed and cared in accordance with the American Association for Accreditation of Laboratory Animal Care standards in AAALAC accredited facilities, and all animal procedures were performed according to protocols approved by the Institutional Animal Care and Use Committees of the National Cancer Institute, National Institutes of Health.

Processing of lymph nodes

Upon receipt of tissue, LNs were washed once in ice cold PBS. After careful removal of surrounding fatty tissue, LNs were cut into 1 mm × 1 mm tissue blocks and digested with collagenase IV (5 mg ml^{-1} in RPMI) (GIBCO) supplemented with 0.5% fatty acid-free BSA (Sigma-Aldrich) and 200 $\mu\text{g ml}^{-1}$ DNase I (Roche). Collagenase-digested tissues were then mechanically digested with a motorized pestle, and the liberated cell suspensions were placed through a 40-micron nylon mesh and washed once in RPMI 1640. These LNMCs were then cryopreserved and used for the different assays.

Processing of tonsils

Tonsils were dissected into small fragments and the pieces were subsequently minced by mechanical disruption between two fully frosted glass slides in complete RPMI 1640 media. Cells were then collected and filtered through a 70 μm nylon membrane mesh and washed in complete media. TMNCs were then separated by Ficoll-density centrifugation. TMNCs were removed and washed twice in complete RPMI 1640 media. Cells were then cryopreserved for subsequent use.

Immunohistochemistry

Immunohistochemistry for mouse anti-PDL1 (clone 339.7G11) (kind gift from Gordon Freeman) and rabbit monoclonal anti-CD23 (clone SP23; Lab Vision, Thermo Fisher Scientific, Inc) was performed using a biotin-free polymer approach (Mouse or Rabbit Polink-2, Golden Bridge International, Inc.) on 5 μm tissue sections mounted on glass slides, which were dewaxed and rehydrated with double-distilled H_2O . Antigen retrieval was performed by heating sections in 0.01% citraconic anhydride in a pressure cooker set at 125 $^{\circ}\text{C}$ for 30 s. Slides were rinsed in ddH_2O , blocked in 0.25% casein and incubated with either diluted mouse anti-PDL1 (1:100; 7 $\mu\text{g mL}^{-1}$) or rabbit anti-CD23 (1:100) in diluent (1x TBS with 0.05% Tween-20 and 0.25% casein) overnight at 4 $^{\circ}\text{C}$. Tissue sections were rinsed in wash buffer (1x TBS containing 0.05% Tween-20) for 10 min followed by an endogenous peroxidase blocking step using 1.5% (v/v) H_2O_2 in TBS (pH 7.4) for 10 min and place in wash buffer. Slides were incubated with Mouse or Rabbit Polink-2 HRP polymer staining system (Golden Bridge International, Inc) according to manufacturer's recommendations (30 min at room temperature) followed by rinsing in wash buffer. Tissue sections were developed with Impact^(TM) 3,3'-diaminobenzidine (Vector Laboratories), counterstained with Hematoxylin and mounted in Permount (Fisher Scientific). Representative images were acquired using a Nikon 80i bright field microscope. Scale bar, 50 μm .

Antibodies

The following fluorochrome-conjugated antibodies were used: anti-human CD3 (clone UCHT1, 1:200), anti-human CD4 (clone RPA-T4, 1:200), anti-human CD19 (clone HIB19, 1:100), anti-human CD27 (clone O323, 1:100), anti-human CD38 (clone HIT2, 1:100), anti-human CD95 (clone DX2, 1:100), anti-human ICOS (clone C398.4A, 1:100), anti-human CD40L (clone 24-31, 1:10), anti-human PD-1 (clone EH12.2H7, 1:100) (all from BioLegend). Additional antibodies were: anti-human CXCR5 (clone RF8 B2, 1:200), anti-human Bcl-6 (clone K112-91, 1:20), anti-human IgD (clone IA6-2, 1:50), anti-human Ki-67 (MOPC-21, 1:10), anti-human PD-L1 (clone MIH1, 1:20), anti-human PD-L2 (clone MIH18, 1:10) from BD Biosciences and anti-human CD45RA (clone 2H4LDH11LDB9, 1:200) from Beckman Coulter. LIVE/DEAD[®] Fixable Dead Cell Stain from Invitrogen was used to gate on live cells as well as Annexin V from BD Biosciences.

For the generation of beads the CELLection[™] Pan Mouse IgG kit was used (Life Technologies 11531D). To coat the beads purified mouse anti-human CD3 (clone UCHT1) and anti-human CD28 (clone CD28.2) from BD Biosciences was used. For isotype control to chimeric murine IgG2a human PD-L1 (kind gift from Gordon Freeman), mouse IgG2a isotype control (M5409) from Sigma-Aldrich was used.

Cell sorting

For isolation of T cell and B cell subsets, LMNCs were thawed and stained with ViViD, CD3 A700, CD4 APC H7, CD45RA ECD, CXCR5 AlexaFluor647, CD19 PE Cy7 and CD27 FITC- specific antibodies at to 4 $^{\circ}\text{C}$ for 20 min before sorting to obtain highly enriched Tfh cells ViViD⁻CD3⁺CD4⁺CD45RA⁻CXCR5^{hi}, non-Tfh cells ViViD⁻CD3⁺CD4⁺CD45RA⁻CXCR5⁻, ViViD⁻CD3⁺CD4⁺CD45RA⁺ and GC-enriched B cells ViViD⁻CD3⁻CD19⁺CD27⁺. Cells were sorted using a BD FACSAria[™] II (BD Biosciences).

Coculture assay

Sorted (2×10^4) GC-enriched B cells were cocultured with Tfh (ViViD⁻CD3⁺CD4⁺CD45RA⁻CXCR5^{hi}) or non-Tfh (CD3⁺CD4⁺CD45RA⁻CXCR5⁻ or CD3⁺CD4⁺CD45RA⁺) cells at a 1:1 ratio in the presence of 100 ng mL^{-1} of staphylococcal

enterotoxin B (SEB) in 96-well V-bottom plates. Supernatants and cells were harvested on day 7 to analyze by ELISA the total levels of IgG and cell viability by flow cytometry and trypan blue exclusion counting to obtain absolute numbers. For cocultures with antigen specific stimulation sorted Tfh cells were cultured with GC-enriched B cells and primed CD14⁺ monocytes (Gag and Env peptide pools) at a 1:1:1 ratio (3×10^4 cells each) for 7 days in 96-well V-bottom plates. The monocytes were obtained by negative selection using magnetic beads (StemCell Technologies) from autologous PBMCs. The HIV-1 consensus B Gag and Env 15 amino acid peptide pools with 11 amino acid overlaps were obtained through the NIH AIDS Research and Reference Reagent Program, Division of AIDS, NIAID, NIH (Cat# 9480 and 8117). Isolated monocytes were allowed to rest for 1 h at 37 °C and primed for 2 h at 37 °C followed by addition to the cocultures. For all coculture experiments a titrated amount (to prevent virus replication without affecting cell viability) of AZT (180nM) was added at the onset of the experiment. For the PD-L1 and PD-L2 blocking experiments 20 $\mu\text{g ml}^{-1}$ of anti-human PD-L1 and PD-L2 blocking antibodies or isotype control (eBioscience) were added at the onset of the coculture for 20 min at 37 °C prior to the addition of Tfh cells.

PD-1 triggering with beads

Purified mouse anti-human CD3, mouse anti-human CD28 (BD Biosciences), chimeric murine IgG2a human PD-L1 (kind gift from Gordon Freeman) or isotype control (murine IgG2a) (Sigma-Aldrich) were covalently attached to CELLection™ Pan Mouse IgG Dynabeads® (Invitrogen). For 2×10^7 beads a total concentration of 140 ng of anti-human CD3, 33 ng of anti-human CD28 and 500 ng of PD-L1 ligand (or isotype control) was used. A total of 2×10^5 sorted Tfh cells (CXCR5^{hi}) were cultured in the presence of beads (PD-L1, control IgG2a or left unstimulated) for 3 days. A total ratio of 2 beads cell⁻¹ was used. Cells were then collected for analysis by flow cytometry and the culture supernatants used for detection of cytokines by ELISA or CBA.

ELISA

96-well Immulon 2HB plates (Thermo Scientific) were coated overnight at 4 °C with monoclonal anti-human IgG (Mabtech, clone MT91/145) antibodies at a concentration of 1 $\mu\text{g ml}^{-1}$ in carbonate bi-carbonate buffer. Plates were washed 5 times with PBS + 0.05% tween-20 in the following day. Plates were subsequently blocked for 1 h with PBS + 10% FBS at RT. Plates were then washed and the culture supernatants added at different dilutions for 1 h at RT. After washing the plates these were incubated with 1 $\mu\text{g ml}^{-1}$ of anti-human IgG-biotin (Mabtech, clone MT78/145) for 1 h at RT. The plates were then washed and incubated with streptavidin-HRP (Mabtech) for 45 min at RT. Plates were subsequently washed and 100 μl of TMB substrate (Sigma-Aldrich) added until appearance of color. The enzymatic reaction was stopped by adding 50 μl of 1M H₃PO₄. The OD (450 nm) was then measured using a SpectraMax plus 384-plate reader (Molecular Devices).

Luminex and CBA

Sorted CD4 T-cell populations were stimulated with phorbol myristate acetate (PMA; 100 ng mL⁻¹; Sigma-aldrich, USA) and Ionomycin (1 $\mu\text{g mL}^{-1}$) (Sigma-Aldrich) in complete RPMI (18 h, 37 °C, 5% CO₂). Supernatants were then collected and analyzed for the presence of cytokines by Luminex (Millipore) following the manufacturer's protocol. For Cytometric Bead Assay (CBA) analysis, supernatants from the cocultures were collected and prepared according to the manufacturer's protocol (BD Biosciences).

Statistical analysis

All statistical analyses were performed using the non-parametric Mann-Whitney test, assuming independent samples. This test uses the rank of the data rather than their raw values to calculate the statistical significance and is an alternative to the *t*-test, when the assumption of normality is not satisfied or could not be tested in the case of small sample sizes. When comparing supplementation of cocultures with IL-21 or PD-1 triggering on Tfh cells by using the bead system the paired Student's *t*-test assay was used as these samples were paired to their control groups. When comparing the % of IgG with respect to HIV⁻ LNs the Wilcoxon signed rank column test was used. In this study, *P*-values of less than 0.05 were considered significant.

Supplementary Material

Refer to Web version on PubMed Central for supplementary material.

Acknowledgments

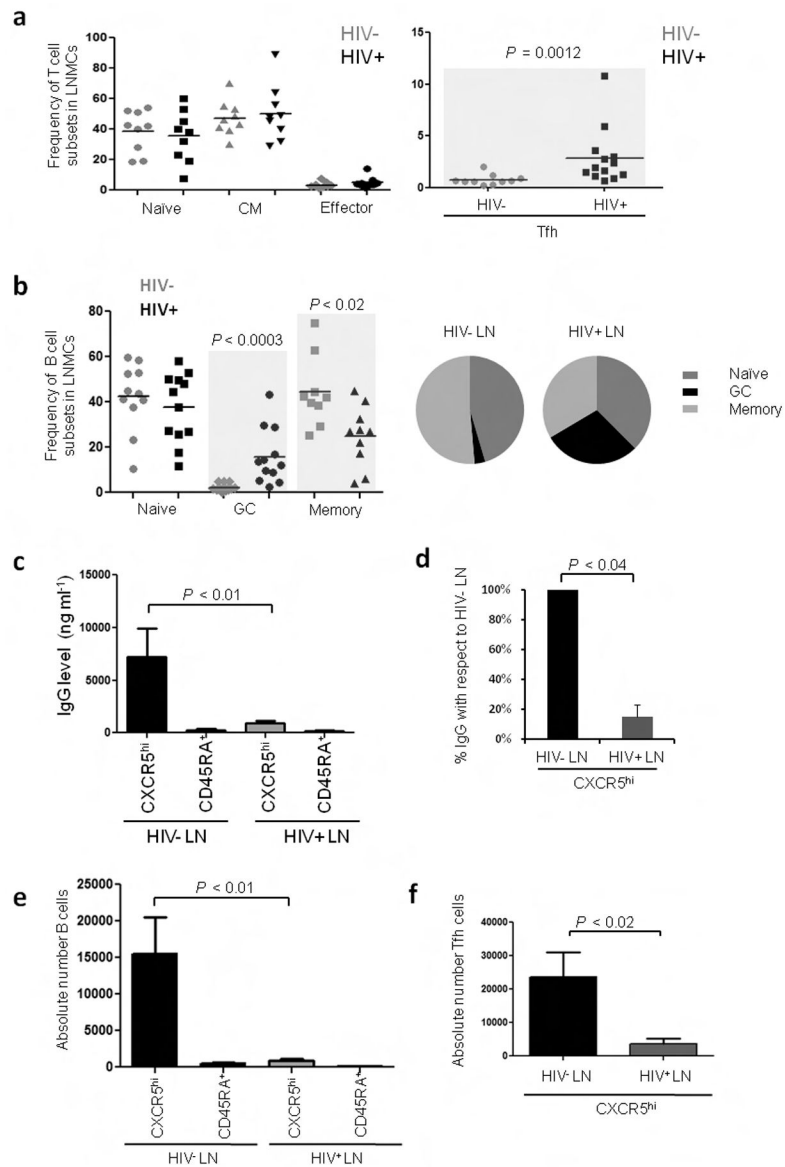
We thank Wendy Ryzner, Rebeka Bordi and Dawn Brown for sample collection. We also thank Kim Kusser and Yu Shi from the Flow Cytometry Core at VGTI-FL for their help with sorting all the samples. We are grateful to Dr. Roberto Debernardo for obtaining the HIV uninfected LNs and to Dr. Benigno Rodriguez for his help with the infected LN samples. This study was supported in part by NIH contract HHSN272201100017C.

References

1. De Milito A, et al. Mechanisms of hypergammaglobulinemia and impaired antigen-specific humoral immunity in HIV-1 infection. *Blood*. 2004; 103:2180–2186. [PubMed: 14604962]
2. Titanji K, et al. Loss of memory B cells impairs maintenance of long-term serologic memory during HIV-1 infection. *Blood*. 2006; 108:1580–1587. [PubMed: 16645169]
3. Hart M, et al. Loss of discrete memory B cell subsets is associated with impaired immunization responses in HIV-1 infection and may be a risk factor for invasive pneumococcal disease. *J Immunol*. 2007; 178:8212–8220. [PubMed: 17548660]
4. Moir S, Fauci AS. B cells in HIV infection and disease. *Nat Rev Immunol*. 2009; 9:235–245. [PubMed: 19319142]
5. van Grevenynghe J, et al. Loss of memory B cells during chronic HIV infection is driven by Foxo3a- and TRAIL-mediated apoptosis. *J Clin Invest*. 2011; 121:3877–3888. [PubMed: 21926463]
6. De Milito A, Morch C, Sonnerborg A, Chiodi F. Loss of memory (CD27) B lymphocytes in HIV-1 infection. *Aids*. 2001; 15:957–964. [PubMed: 11399977]
7. Scheid JF, et al. Broad diversity of neutralizing antibodies isolated from memory B cells in HIV-infected individuals. *Nature*. 2009; 458:636–640. [PubMed: 19287373]
8. Walker LM, et al. Broad neutralization coverage of HIV by multiple highly potent antibodies. *Nature*. 2011; 477:466–470. [PubMed: 21849977]
9. Wu X, et al. Rational design of envelope identifies broadly neutralizing human monoclonal antibodies to HIV-1. *Science*. 2010; 329:856–861. [PubMed: 20616233]
10. Fahey LM, et al. Viral persistence redirects CD4 T cell differentiation toward T follicular helper cells. *J Exp Med*. 2011; 208:987–999. [PubMed: 21536743]
11. Harker JA, Lewis GM, Mack L, Zuniga EI. Late interleukin-6 escalates T follicular helper cell responses and controls a chronic viral infection. *Science*. 2011; 334:825–829. [PubMed: 21960530]
12. Crotty S. Follicular helper CD4 T cells (TFH). *Annu Rev Immunol*. 2011; 29:621–663. [PubMed: 21314428]
13. Haase AT, et al. Quantitative image analysis of HIV-1 infection in lymphoid tissue. *Science*. 1996; 274:985–989. [PubMed: 8875941]
14. Keele BF, et al. Characterization of the follicular dendritic cell reservoir of human immunodeficiency virus type 1. *J Virol*. 2008; 82:5548–5561. [PubMed: 18385252]

15. Lindqvist M, et al. Expansion of HIV-specific T follicular helper cells in chronic HIV infection. *J Clin Invest.* 2012; 122:3271–3280. [PubMed: 22922259]
16. Hong JJ, Amancha PK, Rogers K, Ansari AA, Villinger F. Spatial alterations between CD4(+) T follicular helper, B, and CD8(+) T cells during simian immunodeficiency virus infection: T/B cell homeostasis, activation, and potential mechanism for viral escape. *J Immunol.* 2012; 188:3247–3256. [PubMed: 22387550]
17. Petrovas C, et al. CD4 T follicular helper cell dynamics during SIV infection. *J Clin Invest.* 2012; 122:3281–3294. [PubMed: 22922258]
18. Popovic M, et al. Persistence of HIV-1 structural proteins and glycoproteins in lymph nodes of patients under highly active antiretroviral therapy. *Proc Natl Acad Sci U S A.* 2005; 102:14807–14812. [PubMed: 16199516]
19. Moir S, et al. Evidence for HIV-associated B cell exhaustion in a dysfunctional memory B cell compartment in HIV-infected viremic individuals. *J Exp Med.* 2008; 205:1797–1805. [PubMed: 18625747]
20. Malaspina A, et al. CpG oligonucleotides enhance proliferative and effector responses of B Cells in HIV-infected individuals. *J Immunol.* 2008; 181:1199–1206. [PubMed: 18606673]
21. Karnowski A, et al. B and T cells collaborate in antiviral responses via IL-6, IL-21, and transcriptional activator and coactivator, Oct2 and OBF-1. *J Exp Med.* 2012
22. Choi YS, et al. ICOS receptor instructs T follicular helper cell versus effector cell differentiation via induction of the transcriptional repressor Bcl6. *Immunity.* 2011; 34:932–946. [PubMed: 21636296]
23. Konforte D, Simard N, Paige CJ. IL-21: an executor of B cell fate. *J Immunol.* 2009; 182:1781–1787. [PubMed: 19201828]
24. Sage PT, Francisco LM, Carman CV, Sharpe AH. The receptor PD-1 controls follicular regulatory T cells in the lymph nodes and blood. *Nat Immunol.* 2012
25. Linterman MA, et al. Foxp3+ follicular regulatory T cells control the germinal center response. *Nat Med.* 2011; 17:975–982. [PubMed: 21785433]
26. Chung Y, et al. Follicular regulatory T cells expressing Foxp3 and Bcl-6 suppress germinal center reactions. *Nat Med.* 2011; 17:983–988. [PubMed: 21785430]
27. Wollenberg I, et al. Regulation of the germinal center reaction by Foxp3+ follicular regulatory T cells. *J Immunol.* 2011; 187:4553–4560. [PubMed: 21984700]
28. Hams E, et al. Blockade of B7-H1 (programmed death ligand 1) enhances humoral immunity by positively regulating the generation of T follicular helper cells. *J Immunol.* 2011; 186:5648–5655. [PubMed: 21490158]
29. Bauquet AT, et al. The costimulatory molecule ICOS regulates the expression of c-Maf and IL-21 in the development of follicular T helper cells and TH-17 cells. *Nat Immunol.* 2009; 10:167–175. [PubMed: 19098919]
30. Kroenke MA, et al. Bcl6 and Maf cooperate to instruct human follicular helper CD4 T cell differentiation. *J Immunol.* 2012; 188:3734–3744. [PubMed: 22427637]
31. Kim JI, Ho IC, Grusby MJ, Glimcher LH. The transcription factor c-Maf controls the production of interleukin-4 but not other Th2 cytokines. *Immunity.* 1999; 10:745–751. [PubMed: 10403649]
32. Iannello A, et al. Decreased levels of circulating IL-21 in HIV-infected AIDS patients: correlation with CD4+ T-cell counts. *Viral Immunol.* 2008; 21:385–388. [PubMed: 18788946]
33. Wei X, et al. Antibody neutralization and escape by HIV-1. *Nature.* 2003; 422:307–312. [PubMed: 12646921]
34. Francisco LM, Sage PT, Sharpe AH. The PD-1 pathway in tolerance and autoimmunity. *Immunol Rev.* 2010; 236:219–242. [PubMed: 20636820]
35. Butler NS, et al. Therapeutic blockade of PD-L1 and LAG-3 rapidly clears established blood-stage *Plasmodium* infection. *Nat Immunol.* 2012; 13:188–195. [PubMed: 22157630]
36. Velu V, et al. Enhancing SIV-specific immunity in vivo by PD-1 blockade. *Nature.* 2009; 458:206–210. [PubMed: 19078956]

37. Bekker V, et al. Persistent humoral immune defect in highly active antiretroviral therapy-treated children with HIV-1 infection: loss of specific antibodies against attenuated vaccine strains and natural viral infection. *Pediatrics*. 2006; 118:e315–322. [PubMed: 16847077]
38. Mehta N, et al. Impaired generation of hepatitis B virus-specific memory B cells in HIV infected individuals following vaccination. *Vaccine*. 2010; 28:3672–3678. [PubMed: 20356567]
39. Schacker TW, et al. Collagen deposition in HIV-1 infected lymphatic tissues and T cell homeostasis. *J Clin Invest*. 2002; 110:1133–1139. [PubMed: 12393849]

**Figure 1.**

Tfh cells from HIV-infected subjects are unable to provide appropriate B cell help. **(a)** Frequency of T cell and B cell subsets in LNMCs from HIV⁻ and HIV⁺ subjects. T cell subsets were defined as: naïve (CD3⁺CD4⁺CD45RA⁺CD27⁺), central memory (CD3⁺CD4⁺CD45RA⁻CD27⁺), effector cells (CD3⁺CD4⁺CD45RA⁻CD27⁻) and Tfh cells (CD3⁺CD4⁺CD45RA⁻CXCR5^{hi}). **(b)** B cell subsets were defined as: naïve (CD3⁻CD19⁺CD38⁻IgD⁺), GC (CD3⁻CD19⁺CD38⁺⁺IgD⁻) and total memory B cells (CD3⁻CD19⁺CD38^{+/-}IgD⁻). For T cell subsets (HIV⁻ n=9; HIV⁺ n=9) for Tfh cell subset (HIV⁻ n=10; HIV⁺ n=13) for B cell subsets (HIV⁻ n=11; HIV⁺ n=12). **(c)** IgG production (ng ml^{-1}) in cocultures from LNMCs of HIV⁻ and HIV⁺ subjects after 7 d (HIV⁻ n=6; HIV⁺ n=6) as measured by ELISA. **(d)** Percent difference in the levels of secreted IgG from cocultures of Tfh cells and GC-enriched B cells from HIV⁺ LNMCs when compared to uninfected controls (HIV⁻ n=6; HIV⁺ n=6). **(e)** Absolute number of B cells in coculture with Tfh and non-Tfh cells (HIV⁻ n=6; HIV⁺ n=6) **(f)** Absolute number of Tfh cells after 7 d (HIV⁻ n=6; HIV⁺ n=6) in coculture.

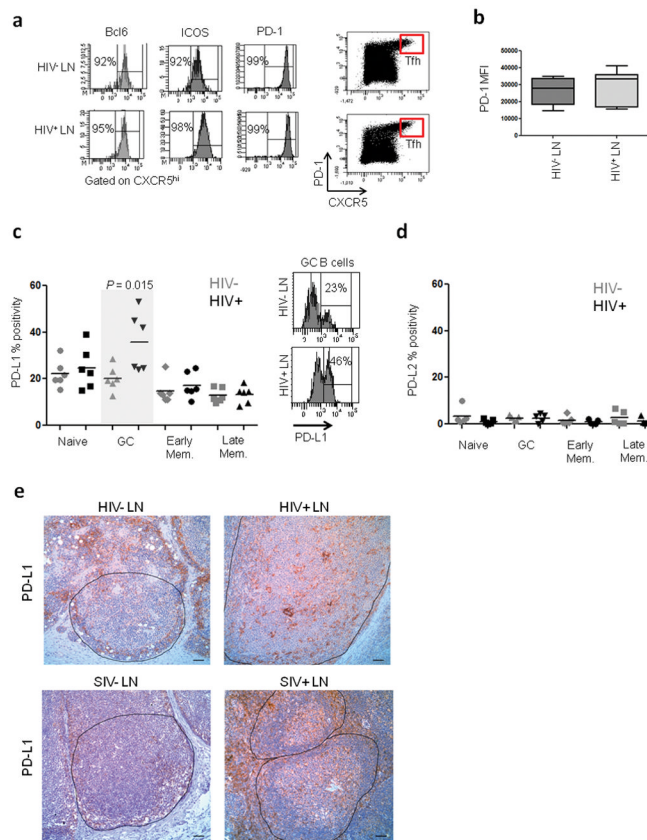


Figure 2.

Ex-vivo characterization of Tfh cells and B cells in LNs from HIV-infected and uninfected individuals. **(a)** Enrichment of Tfh cells in the CXCR5^{hi} population of both HIV⁻ and HIV⁺ LNMCs as determined by Bcl-6, ICOS and PD-1 staining. **(b)** Expression levels of PD-1 on Tfh cells from HIV⁻ and HIV⁺ LNMCs as measured by mean fluorescence intensity (MFI). **(c)** Frequency of PD-L1 expression on B cell subsets from infected and uninfected LNMCs. Subsets were defined as naïve (CD3⁻CD19⁺CD38⁻IgD⁺), GC (CD3⁻CD19⁺CD38^{hi}IgD⁻), early memory (CD3⁻CD19⁺CD38⁺IgD⁻) and late memory (CD3⁻CD19⁺CD38⁻IgD⁻) (HIV⁻ n=6; HIV⁺ n=6). **(d)** Frequency of PD-L2 expression on B cell subsets (HIV⁻ n=5; HIV⁺ n=5). **(e)** Representative images for PD-L1 staining on LN sections from HIV-uninfected (n=6) and infected (n=5) subjects as well as SIV-uninfected (n=4) and infected (n=2) macaques. Scale bar, 50 μ m.

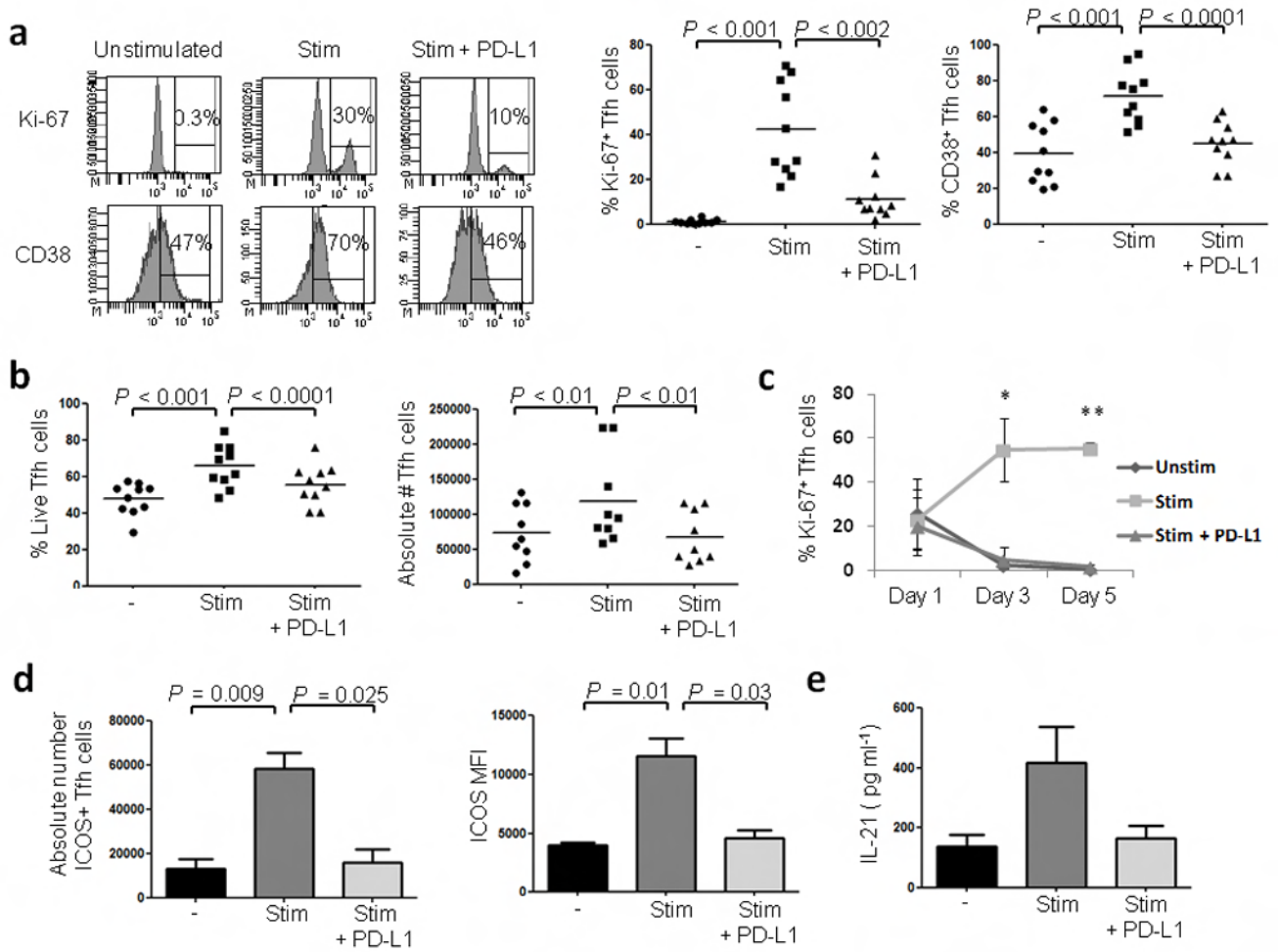


Figure 3. Triggering PD-1 on Tfh cells leads to a decrease in cell proliferation, activation and cytokine secretion. Tfh cells from tonsil mononuclear cells (TMNCs) of uninfected individuals were cultured for 3 d in the presence of anti-CD3, anti-CD28 and isotype coated beads (Stim), anti-CD3, anti-CD28 and PD-L1 coated beads (Stim + PD-L1) or left unstimulated (Unstim). **(a)** Frequency of Ki-67 and CD38 expression on Bcl-6⁺ Tfh cells. The dot plots depict the percent of Ki-67⁺ and CD38⁺ Tfh cells after stimulation with the beads (n=10). **(b)** Effect of PD-1 triggering on the frequency and absolute number of live Tfh cells (n=10) **(c)** Percent of Ki-67⁺ Bcl-6⁺ Tfh cells at different time points after stimulation with the beads (n=3; **P* < 0.01; ***P* < 0.001 between control and PD-L1 beads). **(d)** Effect of PD-1 triggering on the absolute number of ICOS⁺ Tfh cells and ICOS MFI (n=5). Results are representative of two independent experiments **(e)** Effect of PD-1 triggering on IL-21 secretion as measured by ELISA on day 3 (n=4).

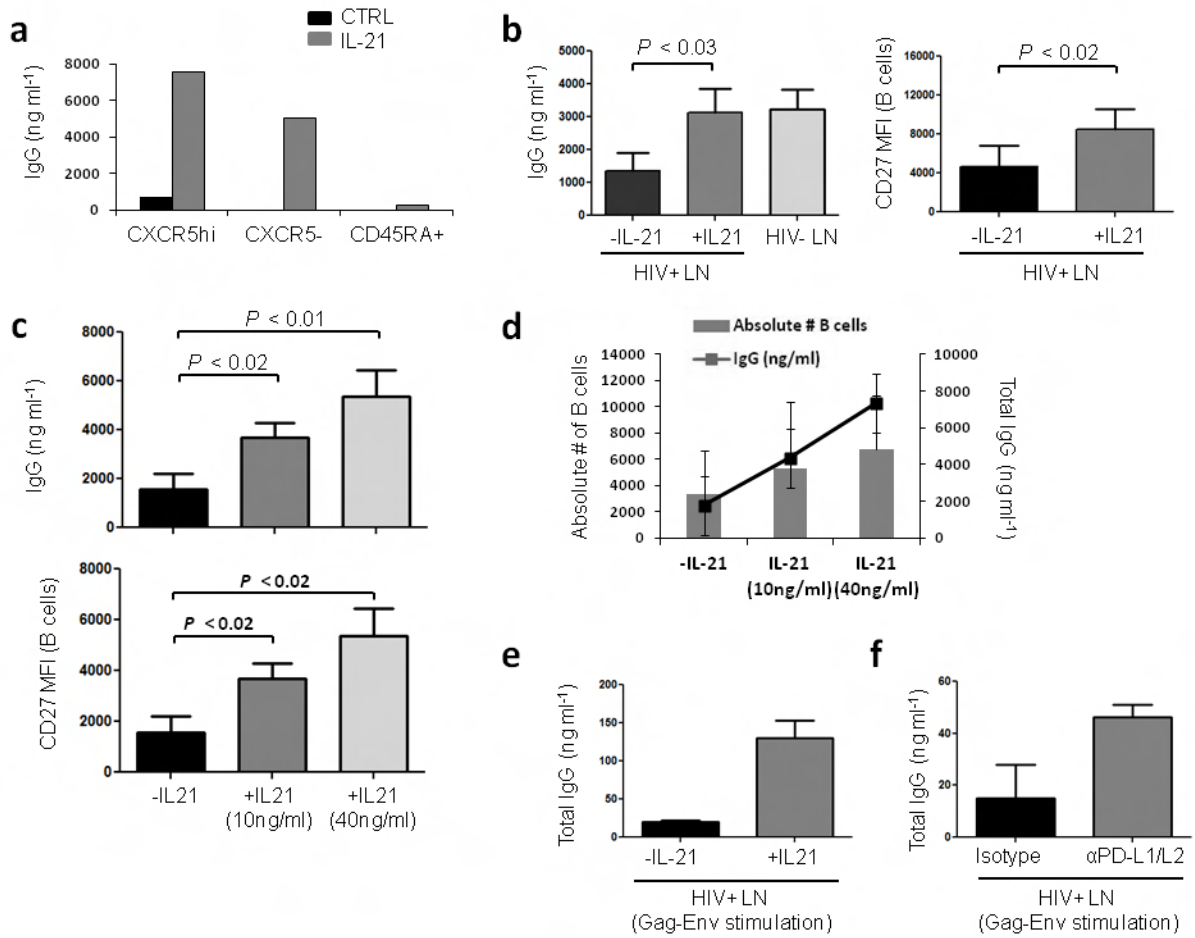


Figure 4. Supplementation with IL-21 restores IgG production in co-cultures from HIV-infected LNMs. **(a)** Representative graph depicting IgG levels in co-cultures of GC-enriched B cells with CXCR5^{hi}, CXCR5⁻ or CD45RA⁺ T cell subsets in the presence of SEB with or without recombinant human IL-21 (10 ng ml⁻¹) after 7 d. **(b)** Increase in IgG production and CD27 MFI on B cells when cocultures of Tfh and GC-enriched B cells from HIV⁺ LNMCs are supplemented with IL-21 (n=5). **(c)** Dose dependent effect of IL-21 on IgG production and CD27 MFI on B cells (n=4). **(d)** Dose dependent effect of IL-21 supplementation on the absolute number of B cells and IgG production in co-cultures of Tfh and GC-enriched B cells from HIV⁺ LNMCs (n=4) after 7 d. **(e)** Effect of IL-21 supplementation on total IgG levels following antigen specific stimulation by culturing Tfh cells and GC-enriched B cells in the presence of primed monocytes after 7 d. (n=2). **(f)** Effect of PD-L1/L2 blocking on IgG production in cocultures of Tfh cells and GC-enriched B cells in the presence of primed monocytes after 7 d (n=2).